Unlocking Access to Enantiopure Fused Uracils by Chemodivergent [4+2] Cross-Cycloadditions: DFT-Supported Homo-Synergistic Organocatalytic Approach

A Journal of the Gesellschaft Deutscher Chemiker

Angewandte International Edition GDCh Chemie

www.angewandte.org

Accepted Article

Title: Unlocking Access to Enantiopure Fused Uracils via Chemodivergent [4 + 2] Cross Cycloadditions: a DFT-Supported Homo-Synergistic Organocatalytic Approach

Authors: Claudio Curti, Gloria Rassu, Marco Lombardo, Vincenzo Zambrano, Luigi Pinna, Lucia Battistini, Andrea Sartori, Giorgio Pelosi, and Franca Zanardi

To be cited as: *Angew. Chem. Int. Ed.* 10.1002/anie.202007509

Link to VoR: https://doi.org/10.1002/anie.202007509

WILEY-VCH

10.1002/anie.202007509

WILEY-VCH

RESEARCH ARTICLE

Unlocking Access to Enantiopure Fused Uracils via Chemodivergent [4 + 2] Cross Cycloadditions: a DFT-Supported Homo-Synergistic Organocatalytic Approach

Claudio Curti,*[a] Gloria Rassu,[b] Marco Lombardo,*[c] Vincenzo Zambrano,[b] Luigi Pinna[d] Lucia Battistini,[a] Andrea Sartori,[a] Giorgio Pelosi,[e] and Franca Zanardi*[a]

[a] Prof. Dr. C. Curti, Prof. Dr. L. Battistini, Prof. Dr. A. Sartori, Prof. Dr. F. Zanardi
Dipartimento di Scienze degli Alimenti e del Farmaco
Università di Parma
Parco Area delle Scienze 27A, 43124 Parma, Italy
E-mail: claudio.curti@unipr.it (C.C.), franca.zanardi@unipr.it (F.Z.)
[b] Dr. G. Rassu, Dr. V. Zambrano
Istituto di Chimica Biomolecolare
Consiglio Nazionale delle Ricerche
Traversa La Crucca 3, 07100 Li Punti Sassari, Italy
[c] Prof. Dr. M. Lombardo
Dipartimento di Chimica "Giacomo Ciamician"
Università di Bologna
Via Selmi 2, 40126 Bologna, Italy
E-mail: marco.lombardo@unibo.it
[d] Prof. Dr. L. Pinna
Dipartimento di Chimica e Farmacia
Università di Sassari
Via Vienna 2, 07100 Sassari, Italy
[e] Prof. Dr. G. Pelosi
Dipartimento di Scienze Chimiche, della Vita e della Sostenibilità Ambientale
Università di Parma
Parco Area delle Scienze 17A, 43124 Parma, Italy

Supporting information for this article is given via a link at the end of the document.

Abstract: The discovery of chemical methods enabling the construction of carbocycle-fused uracils which embody a three-dimensional and functional group-rich architecture is a useful tool in medchem synthesis. In this work, an unprecedented amine-catalyzed [4 + 2] cross cycloaddition is documented, which involved remotely enolizable 6-methyluracil-5-carbaldehydes and β-aryl enals, and chemoselectively produced two novel bicyclic and tricyclic fused uracil chemotypes in good yields and maximum level of enantiocontrol. In-depth mechanistic investigations and control experiments support an intriguing homo-synergistic organocatalytic approach, where the same amine organocatalyst concomitantly engages both aldehyde partners in a first stepwise eliminative [4 + 2] cycloaddition, whose vinylogous iminium ion intermediate product may diverge – depending upon conditions – to either bicyclic targets via hydrolysis, or tricyclic products via a further homo-synergistic trienamine-mediated stepwise [4 + 2] cycloaddition.

Introduction

Over the past two decades, the development of breakthrough synthetic methods, such as organocatalyzed processes and direct activation modalities of nonactivated C-H bonds, have revolutionized the way molecules are imagined and made, with enormous impact on neighboring disciplines including pharmaceutical research and chemical biology.[1] In the drug discovery field, an ever-growing demand for innovative synthesis methods is profiling, enabling the rapid construction of high-quality lead structures that merge the drug-like properties of functionalized core scaffolds with an increased three-dimensional shape, thereby expanding the uncharted chemical space around the putative biological targets.[2]

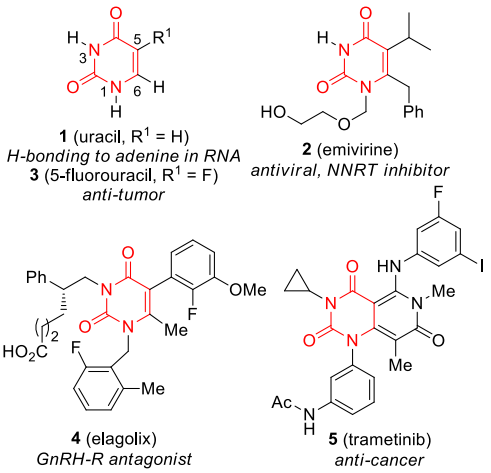

Figure 1. Uracil and examples of uracil-based drugs. NNRT = Non-Nucleoside Reverse Transcriptase.

10.1002/anie.202007509

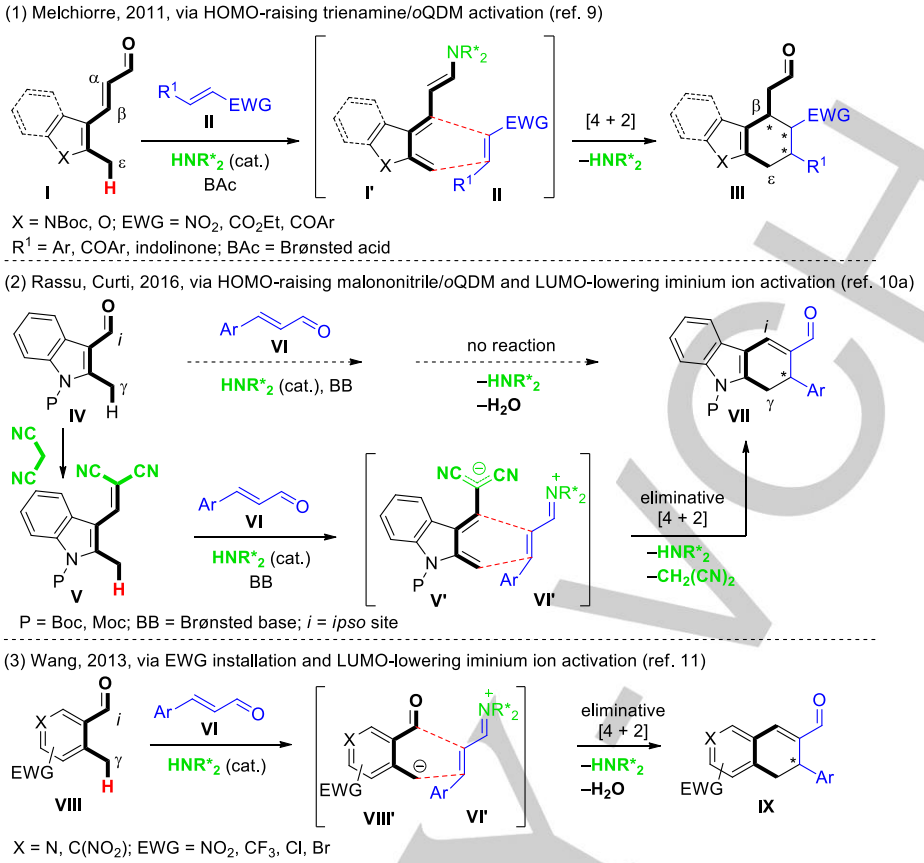

Scheme 1. Previous vinylogous C(sp^3)-H functionalization strategies for the asymmetric construction of fused (hetero)cycles.

Among the privileged core motifs, the naturally occurring heterocycle uracil (compound **1**, Figure 1) occupies a preeminent position, due to its innate chemical structure – a stable six-membered 2,4-pyrimidindione ring with a prevalence of the lactam tautomeric form – responsible for it to establish key gene-related H-bond connections.[3] In addition, uracil has proven to be extremely inclined toward chemical modification, especially at the N1, N3, C5, and C6 positions.[4] Accordingly, a wide array of uracil-based molecules has been accessed so far, exhibiting as many diverse biological activities ranging from antiviral and anti-tumor to herbicidal, bactericidal, and anti-malarial action, as testified by the outstanding number of uracil-founded drugs approved worldwide (Figure 1).[5] Chemical modifications of the uracil ring often maintain the pyrimidindione core, which is enriched with atoms and/or flexible aromatic/aliphatic chains (e.g. compounds **2**, **3**, and **4**), while it is possibly fused with flanking heterocycles, as in the pyridopyrimidine structure **5**, which generally are flattened and C(sp^2)-rich rings.[6] Rare examples of chiral uracil-fused cycles have been reported so far, which have been mainly accessed in racemic format via nonasymmetric syntheses.[5b]

Asymmetric chemical methods enabling the rapid elaboration of commercially available uracil-based materials toward chiral enantio- and functional group-enriched fused uracils are still on demand, and our aim here is to address this goal.

The application of the principle of vinylogy – which states that the electronic properties of a functional group within a molecule are possibly transmitted to a remote position through interposed conjugated multiple bonds – has become an appealing opportunity in organic synthesis for the predictable and selective functionalization of remote C(sp^3)-H bonds.[7] In particular, the benzylic site of *ortho*-methyl (hetero)aromatic carbaldehydes **IV** and **VIII** or extended polyenals of type **I** (Scheme 1) may be envisaged as a remotely enolizable position of the vinylogous aldehyde system, so that useful functionalization chemistry with suitable acceptor components may be fostered. However, deprotonation of these benzylic vinylogous sites is not simple, since it generates highly reactive *ortho*-quinodimethane species (*o*QDMs) – indeed truly polyenolate donors – where the aromatic character of the original ring is temporarily lost.[8] To enhance the acidity of such benzylic protons, clever solutions were devised, as exemplified in Scheme 1. In a first example (Scheme 1, eq. 1),[9] upon condensation of aldehyde **I** with the amine catalyst, the activated *o*QDM-trienamine donor **I′** is formed in situ, which closes with the electron-poor olefin **II** to consign the ε,β-locked fused cyclohexane product **III**. When a similar organocatalyzed reaction was performed using methylindole carbaldehyde **IV** (eq. 2), featuring a formyl function directly attached to the aromatic ring, the cross-coupling with enal acceptor **VI** failed to produce any cyclized products, probably due to insufficient capability of the reaction system to generate the dearomatized *o*QDM donor. In that instance, a strategic *escamotage* was devised, to temporarily activate the donor carbaldehyde chemoselectively as a methylenemalonate derivative **V**, to trigger the intended [4 + 2] coupling between the in situ-activated components **V′** and **VI′**. The spontaneous malononitrile elimination finally provided the

γ,*ipso*-locked cyclohexene aldehyde products **VII** in a global eliminative [4 + 2] cycloaddition reaction.[10]

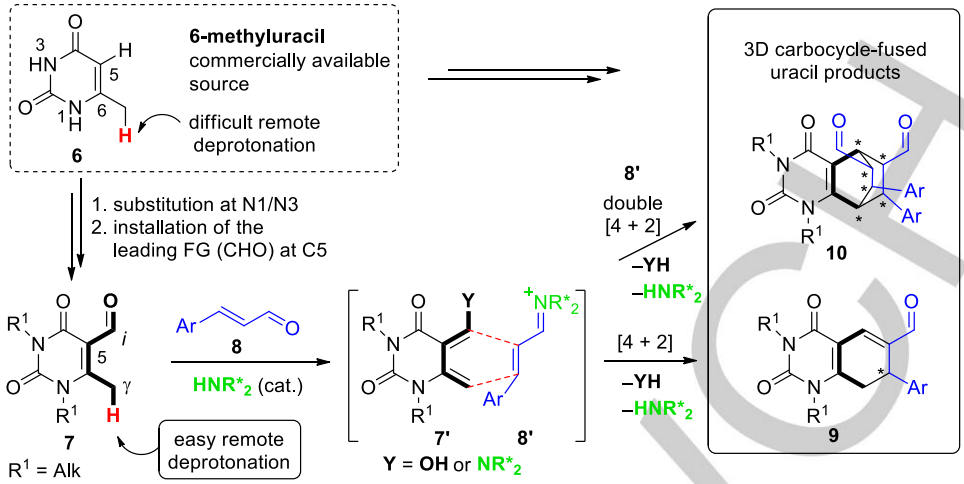

Scheme 2. Projected plan for the asymmetric construction of fused uracils in this work.

In the third example (Scheme 1, eq. 3), the cross-coupling between *ortho*-tolualdehyde **VIII** and enals **VI** could be feasible by installing electron-withdrawing groups in the donor component (i.e. nitro groups); in the event, an eliminative [4 + 2] cyclization took place between **VIII′** and the iminium ion-activated enal partner **VI′**.[11]

In this work, we focus on a novel uracil scaffold, namely compound **7** (Scheme 2), which is easily equipped with an exocyclic carbaldehyde handle at C5 starting from the cheap, commercially available 6-methyluracil precursor **6**. Concomitant vinylogation of the C6-methyl with both the aldehyde and the endocyclic lactam moieties would render the C-H deprotonation at C6 feasible under mild conditions. Remote γ-deprotonation would lead to electron-rich diene **7′**, which is anticipated to undergo either one single or double [4 + 2] cycloadditions with iminium ion-activated dienophile **8′**, to ultimately provide access to diversely shaped chiral carbocyclic uracils of type **9** and/or **10** (vide infra).

Distinguishing features of this strategy are: (1) the exploitation of the unique structural motif of methyluracil carbaldehyde **7**, whose scarce aromatic character would in principle facilitate the formation of the putative active *o*QDM-type species **7′**;[3] (2) the perspective of generating, for the first time, new chiral, 3D space-filling fused uracils in one pot from available uracil-based precursors, representing a step forward with respect to established methods of functionalization of uracils; and (3) the possibility of introducing variable substituents at the N1/N3 atoms, thus allowing modulation of the physico-chemical properties of substrates and targets.

From a mechanistic point of view, additional interesting perspectives would open, as to define the actual role of the amine catalyst in activating *either* or *both* the aldehyde carbonyl groups of the reacting partners **7** and **8**, to unveil the concerted vs stepwise nature of the cyclization reactions, as well as to unravel the intimate reasons responsible for chemodivergency toward either class of uracil-fused products.

Our efforts in this work were directed to put this plan into practice, to demonstrate its viability with diversely substituted substrates, and to get insights into the reaction mechanism via in-depth DFT computational investigation backed up by sound experimental evidence.

Results and Discussion

Synthesis. As a proof of concept of the feasibility of the proposed plan (Scheme 2), we initially evaluated the reaction between *N,N*-dimethyl-substituted methyluracil carbaldehyde **7a** and cinnamaldehyde (**8a**) under amine organocatalysis (Table 1). Compound **7a**, in turn, was accessed via a two-step procedure by starting from cheap and commercially available 6-methyluracil (**6**) via bis-*N*-methylation (Me_2SO_4, K_2CO_3) followed by Vilsmeier formylation. Thus, treating **7a** and **8a** in an equimolar ratio in the presence of popular TMS-protected prolinol **C1** (20 mol%) and catalytic DIPEA in CH_2Cl_2, led to the formation of carbaldehyde **9aa** in 36% yield, accompanied by not negligible amounts of the tricyclic product **10aa** (9% yield; Table 1, entry 1). While compound **9aa** coincided exactly with our expectations according to a plausible eliminative [4 + 2] cross cycloaddition between the two substrates, compound **10aa** came as a surprise, likely as the result of a double cycloadditive process involving two mol equiv of the cinnamaldehyde component (for mechanistic details, see infra). Since the very first experiment, hence, we became aware of three facts: the reaction was feasible, it could lead to two new uracil-fused chemotypes, and the enantiocontrol by secondary amine organocatalysis was excellent for both types. Accordingly, we proceeded to the systematic screening of the reaction conditions, to maximize both yield and chemoselectivity for either target, while maintaining enantiocontrol.

10.1002/anie.202007509

Table 1. Proof of concept of the plan and selected optimization of reaction conditions.[a]

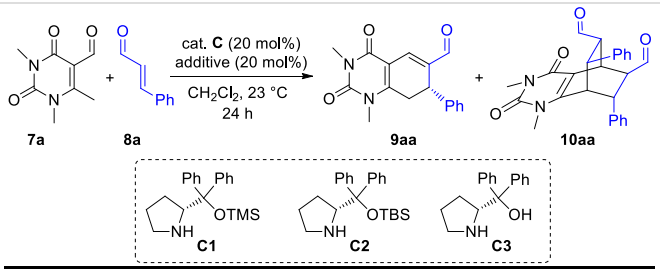

Entry	Cat. **C**	**7a**:**8a**	Additive	Yield[b]	**9aa**:**10aa**[c]	*ee* [%] **9aa/10aa**[d]
1	**C1**	1:1	DIPEA	45	4:1	99/>99
2	**C2**	1:1	DIPEA	30	>10:1	99/n.d.
3	**C3**	1:1	DIPEA	15	n.d.	n.d./n.d.
4	-	1:1	-	-	-	-
5	-	1:1	DIPEA	-	-	-
6[e]	**C1**	1:1	DIPEA	35	1:1	99/>99
7	**C1**	1:1	Et_3N	40	2:1	99/>99
8	**C1**	1:1	-	55	5:1	99/>99
9	**C1**	1.5:1	-	65	10:1	99/n.d.
10[f]	**C1**	1.5:1	-	35	10:1	99/n.d.
11[g]	**C1**	1.5:1	-	15	n.d.	n.d./n.d.
12[h]	**C1**	1.5:1	-	30	>10:1	99/>99
13	**C1**	1.5:1	BA	55	1:1	99/>99
14	**C1**	2:1	-	74	>10:1	>99/n.d.
15	**C1**	1:1.5	-	45	3:1	99/>99
16	**C1**	1:3	BA	79	1:6	n.d./>99

[a]All reactions were run under inert atmosphere on a 0.2 mmol scale (0.1 M). [b]Combined yield of isolated products **9aa** and **10aa**. [c]Determined by ^{1}H NMR analysis of the crude reaction mixture. [d]Determined by HPLC analysis on a chiral stationary phase. [e]Toluene was used. [f]0 °C and 48 h reaction time. [g]50 °C and 12 h reaction time. [h]10 mol% catalyst loading. DIPEA = *N,N*-diisopropylethylamine. BA = benzoic acid. n.d. = not determined. For complete optimization survey, see Tables S1-S2 in the Supporting Information.

As for the organocatalysts screened, the first catalyst used, **C1**, revealed to be the best one, since reactions performed with other secondary amine catalysts or tertiary amine bifunctional catalysts either gave inferior results in terms of product yield (entries 2 and 3), or proved completely non-productive (Table S1, Supporting Information). No reaction took place in the absence of any amine catalyst, both in the presence or absence of the DIPEA additive, emphasizing the key role of the catalyst in triggering the transformation (entries 4 and 5). The role of solvent, additive, molar ratio between substrates, catalyst loading, and reaction temperature was next investigated (Table 1, entries 7-16 and Table S2 in the Supporting Information), ultimately leading to the following conclusions. First, chemodivergency, i.e. **9aa**:**10aa** ratio, was strictly dependent by the **7a**:**8a** substrate ratio, with bicycle **9aa** prevailing with excess of **7a** over **8a**, and tricycle **10aa** predominating with excess **8a** over **7a**. Second, the role of the additive crucially impacted both yield and chemoselectivity; in fact, the absence of any added Brønsted base or acid improved the overall efficiency of the reaction toward the formation of bicycle **9aa**, while catalytic addition of benzoic acid as an additive enhanced the efficiency of the transformation in favor of tricyclic product **10aa**. Lastly, the catalyst loading had to be maintained at 20 mol% level, since lowering the quantity of catalyst heavily impacted the overall efficiency (Table 1, entry 12, and Table S2 in Supporting Information), clearly suggesting clues on the reaction mechanism (see infra).

Overall, the optimized reaction protocol toward bicyclic product **9aa** entailed the use of a 2:1 ratio of *N,N*-dimethyl-substituted **7a** and cinnamaldehyde **8a**, catalyst **C1** with a 20 mol% loading, in the absence of any additives, in dichloromethane at room temperature for 24 h, leading to **9aa** in 68% isolated yield, >10:1 chemoselectivity and >99% ee (Table 1, entry 14).

The optimized procedure to tricyclic product **10aa** called for the use of uracil **7a** and enal **8a** in a 1:3 ratio, using the same catalyst **C1** in 20 mol% loading, with the addition of catalytic benzoic acid (20 mol%) in dichloromethane at room temperature, giving **10aa** in 68% isolated yield, 6:1 chemoselectivity, and >99% ee (Table 1, entry 16).

We next investigated a battery of diversely functionalized substrates **7** and **8** to evaluate the functional group compatibility of the two procedures. Table 2 and Table 3 illustrate the results of this investigation toward bicyclic uracils **9** and tricyclic compounds **10**, respectively. As for the eliminative [4 + 2] cyclization to products **9**, substituted cinnamaldehydes **8** bearing either electron-withdrawing or electron-donating groups proved competent enal substrates in couple with *N,N*-dimethyl uracil **7a**, giving the corresponding bicycles **9ab**, **9ac**, **9ae**, **9af**, and **9ah** in reasonable-to-good isolated yields and excellent enantioselectivities in all cases. The reaction toward **9ab** was repeated on a 5× scale proving equally efficient and enantioselective. Good results were also obtained with naphthyl derivative **9ad** and furyl-equipped compound **9ag**. Inferior performance was instead witnessed using a polyconjugated dienal substrate (namely, 5-phenyl-2,4-pentadienal **8i**), which reacted with **7a** giving bicycle **9ai** in a poor 20% yield, accompanied by preponderant formation (50% yield) of the corresponding aromatized compound (see Supporting Information). In this case, extended double bond conjugation could be responsible for facile oxidation of **9ai** in air during the workup procedure. Variation of the uracil component **7** entailed the use of methoxymethyl- (MOM), methoxyethoxymethyl- (MEM), and benzyloxymethyl- (BOM) substituted uracils **7b**, **7c**, and **7d**, respectively, which were prepared from commercial methyluracil carbaldehyde **6** in three steps (see Supporting Information). These substrates reacted with cinnamaldehyde according to the standard procedure, providing the corresponding products **9ba**, **9ca**, and **9da** in good isolated yields and, again, notable enantiomeric excesses.[12]

As a limitation of the procedure, the reactions failed with *N,N*-unsubstituted uracil substrate (Table 2), mainly due to its very poor solubility in dichloromethane. Also, β-alkyl-substituted enals (e.g. R^2 = cyclohexyl) proved recalcitrant substrates under the reported reaction conditions, even with prolonged reaction times and higher temperatures. In all cases reported in Table 2, chemoselectivity between the expected products **9** and the corresponding tricycles **10** remained at high levels (**9**:**10**, >10:1), as determined by NMR analysis of the crude reaction mixtures.

By simply adjusting the substrate ratio and adding benzoic acid co-catalyst (optimized conditions of Table 1, entry 16), access to variously adorned products **10** was at hand, which remarkably feature a tricyclic skeleton with six contiguous stereocenters. The representative compounds in Table 3 were obtained in good isolated yields, moderate-to-good chemoselectivity (**10**:**9**, 6:1), complete diastereoselectivity, and excellent levels of

10.1002/anie.202007509

WILEY-VCH

enantioselectivity, as detected by chiral HPLC analysis of the corresponding bis-carbinols.

Table 2. Substrate scope for the chemo-, regio-, and enantioselective synthesis of bicyclic uracils **9**.[a]

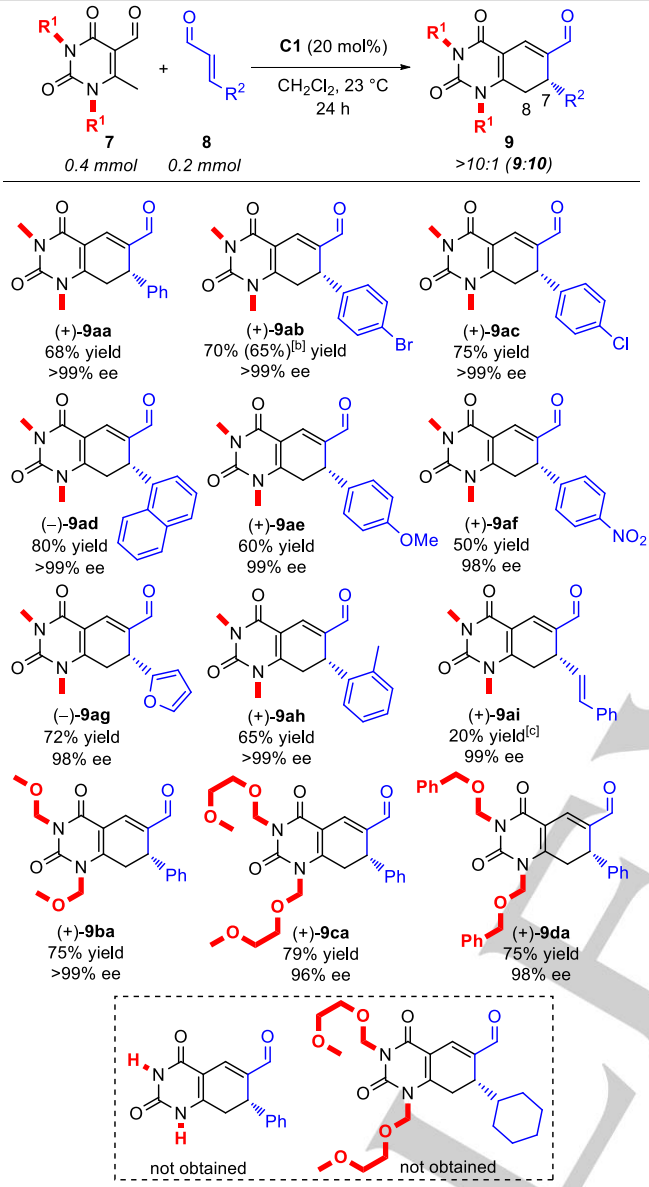

[a] All reactions were run under an inert atmosphere in 0.1 M solutions of dry CH_2Cl_2. Yields refer to isolated products **9**. Enantiomeric excesses (*ee*) were determined by HPLC analysis on a chiral stationary phase. [b] Isolated yield on a 5 × scale. [c] The corresponding aromatized achiral product was isolated in 50% yield. For further details, see the Supporting Information.

The varied functional group pattern of compounds **9** and **10** served for further chemical transformations. Derivatization of aldehyde *ent*-**9ae** into crystalline benzoyl carbinol **11** (Scheme 3, eq. 1), allowed us to determine the absolute configuration of the products indirectly, by single crystal X-ray analysis (see the Supporting Information for details).[13] Further elaborations included carbonyl reduction of products **10** into the corresponding bis-alcohols **12** (Scheme 3, eq. 2), and reductive removal of BOM protections from bis-carbinol **12da** to afford *N,N*-unsubstituted tricycle **13da** (eq. 3).

Table 3. Substrate scope for the chemo-, regio-, diastereo-, and enantioselective synthesis of tricyclic uracils **10**.[a]

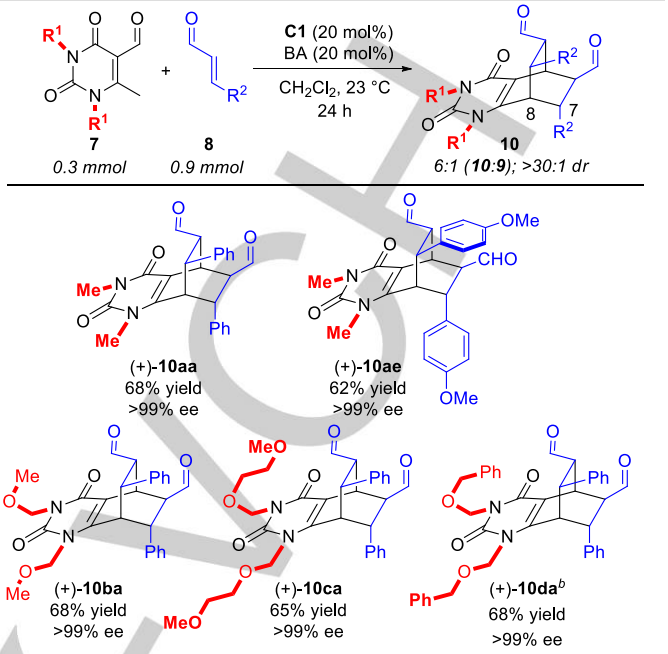

[a] All reactions were run under an inert atmosphere in 0.1 M solutions of dry CH_2Cl_2. Yields refer to isolated products **10**. Diastereomeric ratios (dr) were determined by ^1H NMR analysis of the crude reaction mixtures. Enantiomeric excesses (*ee*) were determined by HPLC analysis of the corresponding bis-alcohols of type **12** (see infra, Scheme 3) using a chiral stationary phase. [b] Relative configuration corroborated by 2D NMR NOESY analysis ($CDCl_3$, 400 MHz). For further details, see the Supporting Information.

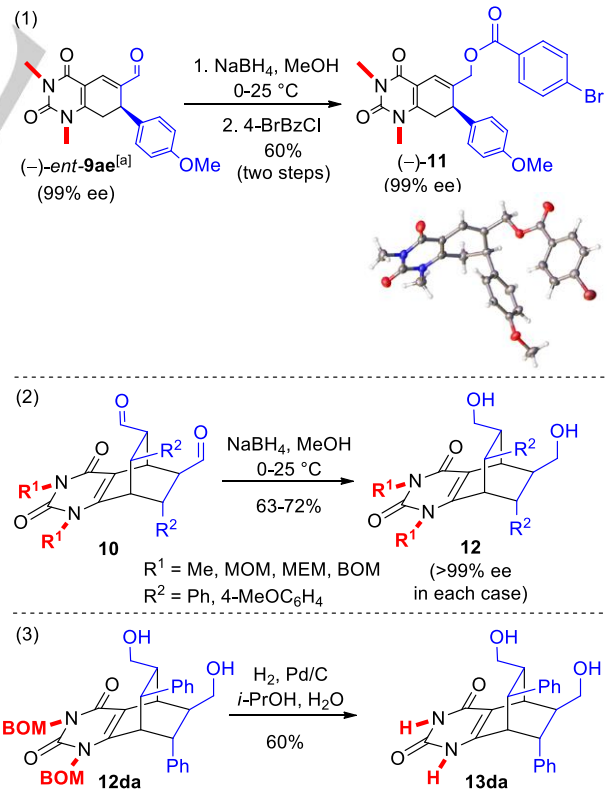

Scheme 3. Chemical elaboration of the fused uracil products. MOM = methoxymethyl, MEM = methoxyethoxymethyl, BOM = benzyloxymethyl. For

10.1002/anie.202007509

experimental details, see the Supporting Information. [a] Obtained from **7a** and *p*-methoxycinnamaldehyde (**8e**) according to the conditions reported in Table 2, using *ent*-**C1** instead of **C1**.

Mechanistic Insights. The chemistry herein disclosed posed questions about the actual mechanism of these transformations, and a special investigation was deserved to unravel three central points: i) *role played by the amine catalyst* in orchestrating the coupling between the substrates; ii) *nature of the eliminative [4 + 2] cross cycloaddition to bicycles* ***9*** (i.e. concerted vs stepwise, catalyst recycling via elimination); iii) *nature of the double [4 + 2] cycloaddition sequence to tricycles* ***10*** and *possible linking between the bicycle/tricycle catalytic cycles.*

i) About the role played by the amine catalyst. From the observed experimental results, we learned that **C1** was an indispensable ingredient for the reaction to occur, enantiocontrol was almost excellent in all cases, and decreasing catalyst loading to less than 20 mol% dramatically lowered the efficiency of the process, giving clues about a double participation of the catalyst in activating both substrates. Given the poorly differentiated nature of the starting reactants **7** and **8** (both α,β-unsaturated aldehydes), it was reasonable to assume a concomitant covalent activation of both **7** and **8** by the aminocatalyst. Organocatalyzed cross- or self-condensations of aldehydes are known in the literature, but in-depth studies supported by calculations and/or experimental evidence about their mechanism are quite rare and could hardly help us in this endeavor.[14] To test the hypothesis that a double activation of reactants by **C1** was operative, a couple of control experiments was carried out, where either of the two reactants was replaced by a non-aldehyde non-activatable congener (Scheme 4, eqs. 1 and 2). Thus, when **7a** was reacted with *E*-nitrostyrene (**14**) in the presence of **C1** (20 mol%), the corresponding bicyclic compound **15** was isolated in 18% yield as a single diastereoisomer (Scheme 4, eq. 1). Incorporation of the catalyst moiety within the framework of the final product clearly established the role of dienamine intermediate **7a-EN** in the addition reaction, thus confirming the hypothesis that uracil-based aldehyde **7a** may be activated by **C1** via dienamine formation. More detailed investigation of this control reaction via DFT calculations[15] showed that this cycloaddition reaction proceeds via a two-step mechanism entailing a first rate- and stereo-determining dienamine-mediated vinylogous Michael reaction to fix the C7-C8 bond, followed by closure of the nitronate intermediate to the evolving iminium ion to install the C5-C6 bond (see Chart S2 in the Supporting Information).

In the second control experiment (Scheme 4, eq. 2), uracil aldehyde **7a** was converted into alkenylidene malononitrile **16a**, which was reacted with cinnamaldehyde **8a** under the usual optimized conditions. In the event, bicyclic product **9aa** was mainly recovered in excellent enantiocontrol (99% *ee*), thus corroborating the hypothesis of an active participation of catalyst **C1** in this reaction, via iminium ion **8a-IM** (in this instance, a [4 + 2] cycloaddition followed by elimination of malononitrile is operative).[10b] Further confirmation of this hypothesis came from DFT calculations, as described in the next paragraph.

ii) About the nature of the eliminative [4 + 2] cross cycloaddition toward bicycles ***9***. Given the reasonable existence of both **7a-EN** and **8a-IM** in the reaction context, we initially modeled the addition reaction of **7a-EN** to the iminium ion **8a-IM** (Chart 1). DFT calculations[15] revealed a two-step reaction mechanism but, contrary to the previously calculated pathway (Scheme 4, eq. 1 and Chart S2 in Supporting Information), now the second C5-C6 bond-forming reaction determines the overall cyclization barrier.

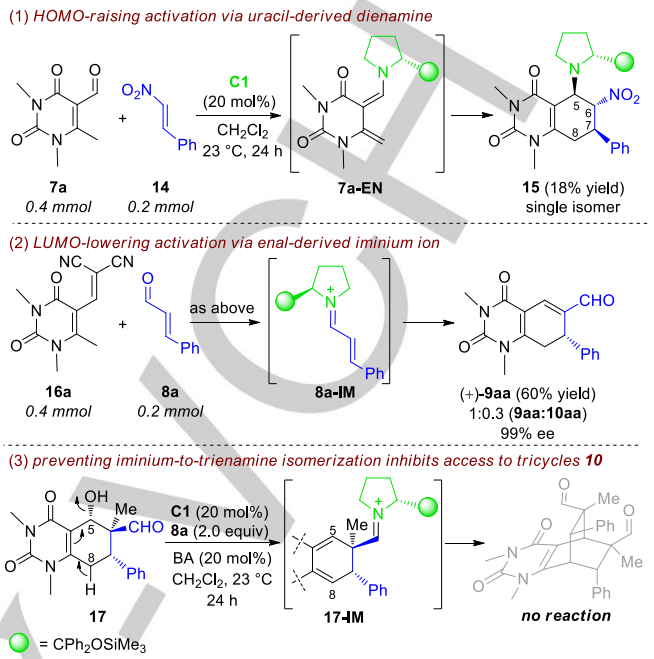

Scheme 4. Control experiments supporting the mechanistic investigation.

In this case, both the dienamine **7a-EN** and the Michael acceptor **8a-IM** possess a single unhindered diastereotopic face available for the addition. As a result, a single approach of the two reagents becomes energetically feasible, determining the (*S*)-absolute configuration of the C7 stereocenter of the target. The reaction profile for the complete cyclization deriving from the most favorable *synclinal* approach of **7a-EN** and **8a-IM** and leading to the iminium ion of the final product **9aa** is reported in Chart 1. The structures of transition states relative to C7-C8 (**TS-I**) and C5-C6 (**TS-II**) bond-forming reactions, as well as the transition state for the elimination reaction (**TS-III**) are also depicted in Chart 1. While the iminium ion moiety within intermediate **I-2a** could be in principle hydrolyzed releasing half of the bound catalyst **C1**, the part directly bound to C5 cannot readily re-enter the catalytic cycle. In order to establish whether the final eliminated product **9aa** could be formed from this intermediate, we tried to model the elimination reaction from the enamine **I-2a-EN** deriving from **I-2a**, but no feasible reaction pathway could be found. Indeed, a possible elimination pathway was found from enamine **I-2a-EN-H$^+$** bearing a protonated pyrrolidine ring at C5 (Chart 1). A possible explanation could be that, even in the absence of acidic additives, *catalytic amounts of protic acids are still present in solution*, due to easy oxidation of the commercially available starting aldehydes.

A second explanation for the different behavior of cinnamaldehyde **8a** with respect to nitrostyrene **14** could be found in the different energetic requirement for the final cyclization step. While the nitronate ion cyclizes almost with no barrier (**I-7** in Chart S2), ring closure of intermediate **I-1a** is considerably more energetically demanding (Chart 1), rendering *iminium ion hydrolysis before the cyclization step* possible.

10.1002/anie.202007509

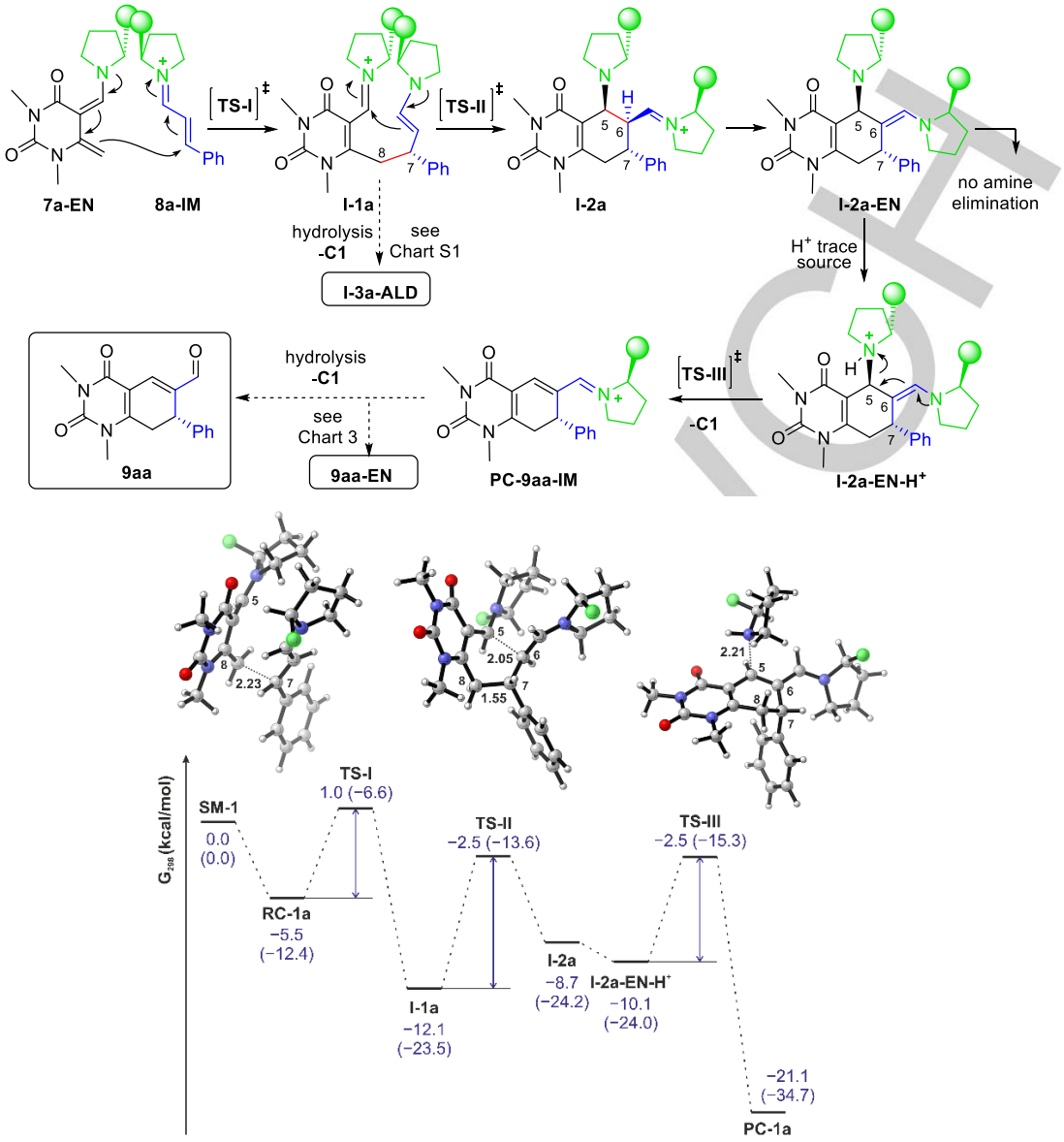

Chart 1. Reaction scheme (above) and reaction profile (below) for the addition of **7a-EN** to **8a-IM**. Free energy profiles (kcal·mol^{-1}) in the gas-phase at the M06-2X/6-31G(d) level of theory. Energies in parentheses are relative to single point calculations at the M06-2X/6-311++G(d,p) level of theory in CH_2Cl_2. **SM-1**: separated reactants at infinite distance (**7a-EN** + **8a-IM**); **RC**: reactant complex; **TS**: transition state; **I**: intermediate; **PC-1a**: product complex (**9aa-IM** + **C1**). Structures of transition states **TS-I** (*synclinal* approach), **TS-II** (cyclization step) and **TS-III** (elimination reaction); distances in Angstrom. Silylated diphenylmethanol group is represented as a green sphere.

To establish whether this last reaction pathway is possible, we modeled the corresponding cyclization/elimination steps on the aldehyde deriving from intermediate **I-1** (**I-3a-ALD,** see Chart S1, Supporting Information). The calculated reaction profiles for the cyclization reactions are in complete accordance with those reported by Houk for the aldol reaction between acetaldehyde and *N*,*N*-dimethylvinylamine.[16] In particular, in the absence of acidic additives, the reaction proceeds to give an oxetane intermediate with a large activation barrier (40.0 kcal·mol^{-1} in the gas phase and 31.6 kcal·mol^{-1} in CH_2Cl_2); on the contrary, in the presence of a protic acid, the cyclization step proceeds promptly without any barrier. Similar to what observed for **I-2a** (Chart 1), no further elimination reaction could be found in the absence of a proton source. Upon protonation of the cyclized alcohol intermediate, a transition state leading to the iminium ion of the final product was easily identified, by starting from either *E*- or *Z*-configured enamine (Chart S1, Supporting Information). Differently from amine elimination, where the iminium ion/enamine conversion was almost an isoergonic transformation (**I-2a**/**I-2a-EN**, Chart 1, ΔG_{298} = –1.4 kcal·mol^{-1} in the gas phase and 0.12 kcal·mol^{-1} in CH_2Cl_2), in this latter case the same conversion was highly endergonic (ΔG_{298} = 22.9/23.3 kcal·mol^{-1} in the gas phase and 20.8/24.7 kcal·mol^{-1} in CH_2Cl_2, for *E*- and the *Z*-enamines, respectively), suggesting a quite large activation barrier.

Finally, to confirm the involvement of **8a-IM** in the reaction course, the addition of **7a-EN** to **8a** was also modeled (Chart 2). In this case, a single-step asynchronous cyclization was found, characterized by a transition state (**TS-IV**) in which the C7-C8

10.1002/anie.202007509

bond is almost formed (2.09 Å), while the C5-C6 bond is considerably longer (2.89 Å). Moreover, the corresponding activation barrier (15.8 kcal·mol^{-1} in the gas phase and 13.6 kcal·mol^{-1} in CH_2Cl_2) resulted more than doubled than that relative to the addition to **8a-IM** (see Chart 1 vs Chart 2).

So far, the calculation results suggested that 1) the *addition reaction involves both the enamine of **7a** and the iminium ion of **8a*** derived from condensation with catalyst **C1**, constituting a perfect yet rare example of a very efficient enantioselective homo-synergistic organocatalytic transformation. Indeed, amine-catalyzed eliminative [4 + 2] cycloadditions were previously reported by Watanabe[14a] and Jorgensen groups,[14c] dealing with self- or cross condensation of linear enals; in those instances, double activation of both substrates via enamine and iminium ion formation with the organocatalyst was postulated, but only a partial investigation of the actual reaction mechanism was documented. 2) The *presence of traces of a protic acid is required* to foster the final elimination reaction, and 3) even if the acid-catalyzed cyclization step involving the aldehyde acceptor is considerably faster than the addition to the corresponding iminium ion (Chart S1 vs Chart 1), the subsequent iminium/enamine isomerization, required for the final elimination step, appears much more energetically favorable in the case of the iminium ion pathway (Chart 1).

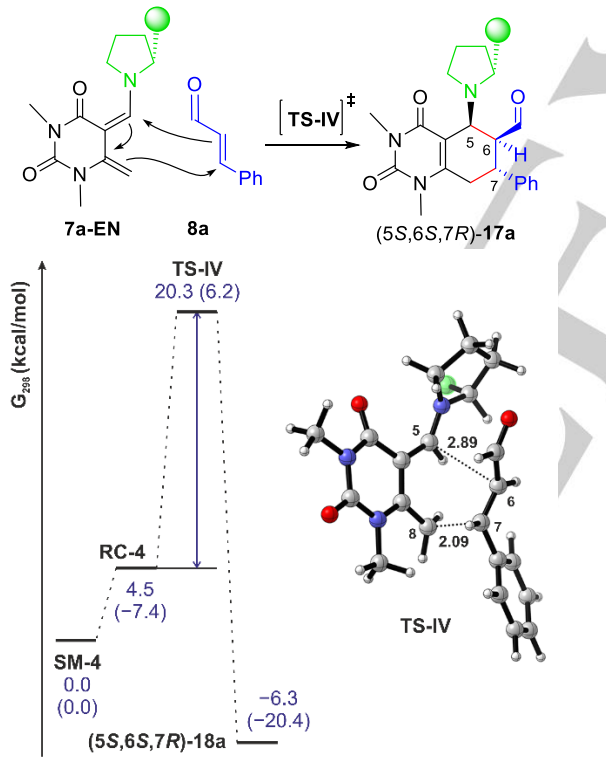

Chart 2. Reaction scheme (above), reaction profile (below, left) for the addition of **7a-EN** to **8a** and structure of transition state **TS-IV** (below, right, distances in Angstrom). Free energy profiles (kcal·mol^{-1}) in the gas-phase at the M06-2X/6-31G(d) level of theory. Energies in parentheses are relative to single point calculations at the M06-2X/6-311++G(d,p) level of theory in CH_2Cl_2. **SM-4**: separated reactants at infinite distance; **RC**: reactant complex; **TS**: transition state. Silylated diphenylmethanol group is represented as a green sphere.

*iii) About the nature of the double [4 + 2] cycloaddition sequence to tricycles **10** and possible linking between the bicycle/tricycle catalytic cycles.* As described in the synthesis paragraph, when the reaction was carried out in the absence of additives and with a slight excess of uracil **7a** (1.5 equiv), product **9aa** was isolated in good overall yield, together with trace amounts of tricyclic adduct **10aa** (Table 2, entry 9, non-optimized conditions). Indeed, when the reaction was carried out in the same conditions in the presence of 20 mol% benzoic acid as an acidic additive (Table 2, entry 13), **9aa** and **10aa** were isolated in comparable yields. These results suggested that **10aa** derives directly from an intermediate involved in the formation of **9aa**. Thus, under optimized conditions (Table 2, entry 16), **10aa** could be isolated as the main reaction product if the catalytic cycle is fostered by an acidic additive and a larger excess of cinnamaldehyde **8a** is used (3 equiv). Considering the mechanistic rationale so far obtained, it seems reasonable to postulate that the trienamine **9aa-EN** - directly deriving by isomerization of the iminium ion **9aa-IM** (the final product in Chart 1) - is involved in a further coupling to the iminium ion of cinnamaldehyde (**8a-IM**), leading to the formation of **10aa** (Chart 3). DFT calculations showed, once more, that this reaction follows a two-step mechanism, where the second step, namely the cyclization reaction, determines the overall reaction barrier. Again, both trienamine **9aa-EN** and the Michael acceptor **8a-IM** have only one unhindered diastereotopic face available for the addition, completely determining the (8*R*,9*S*)-absolute configuration of the newly forged C8 and C9 stereocenters. Accordingly, the second cyclization step fixes the absolute (5*S*,10*S*)-configuration at the C5 and C10 stereocenters in an unequivocal manner. The overall [4 + 2] cycloaddition entails a first trienamine-mediated bisvinylogous Michael reaction, followed by an intramolecular enamine-mediated Michael reaction; in the event, four new contiguous stereocenters are nicely formed with complete absolute stereocontrol. The configuration of the last new stereocenter at the C6 position is determined later, during enamine/iminium ion equilibration to consign the final target **10aa**; the aldehyde substituent at C6 assumes the most thermodynamically stable pseudo-equatorial disposition, thus accounting for the observed 6*S*-absolute configuration for this stereocenter.

Given the above considerations, chemodivergence toward either bicyclic product **9aa** or tricyclic congener **10aa** is established by the presence of the *key oQDM-like trienamine intermediate **9aa-EN*** directly deriving from **9aa-IM**. If conditions are present which favor this isomerization (e.g. protic conditions), the reaction proceeds to tricycle **10aa**, especially when excess of dienophile **8a-IM** is present. On the other hand, if **9aa-IM** is not given the possibility to isomerize to trienamine **9aa-EN**, for instance because it is hydrolyzed to the corresponding aldehyde, then the reaction path stops at this stage consigning bicycles **9**. As a confirmation of this sentence, one further control experiments was carried out (Scheme 4, eq. 3), where bicyclic compound **17**, bearing a quaternary C6 carbon, was reacted with cinnamaldehyde **8a** in the presence of catalyst **C1** and benzoic acid (20 mol% each). In the event, no even minimal conversion of **17** to the corresponding tricyclic compound was witnessed in 24 h. In this case, transformation of **17** to the corresponding *o*QDM would be in principle possible via 5,8-conjugate water elimination, but no isomerization to the trienamine would be feasible due to interruption of conjugation by the quaternary C6 center, with consequent inhibition of the [4 + 2] cyclization to any tricyclic

10.1002/anie.202007509

product. That is to say, *only hypervinylogous enamines of type **9aa-EN** may succeed to forge such complex tricyclic structures, providing chemodivergence.*[17]

An overall depiction of the intertwined catalytic cycles accounting for the transformations outlined in this work is given in Scheme 5.

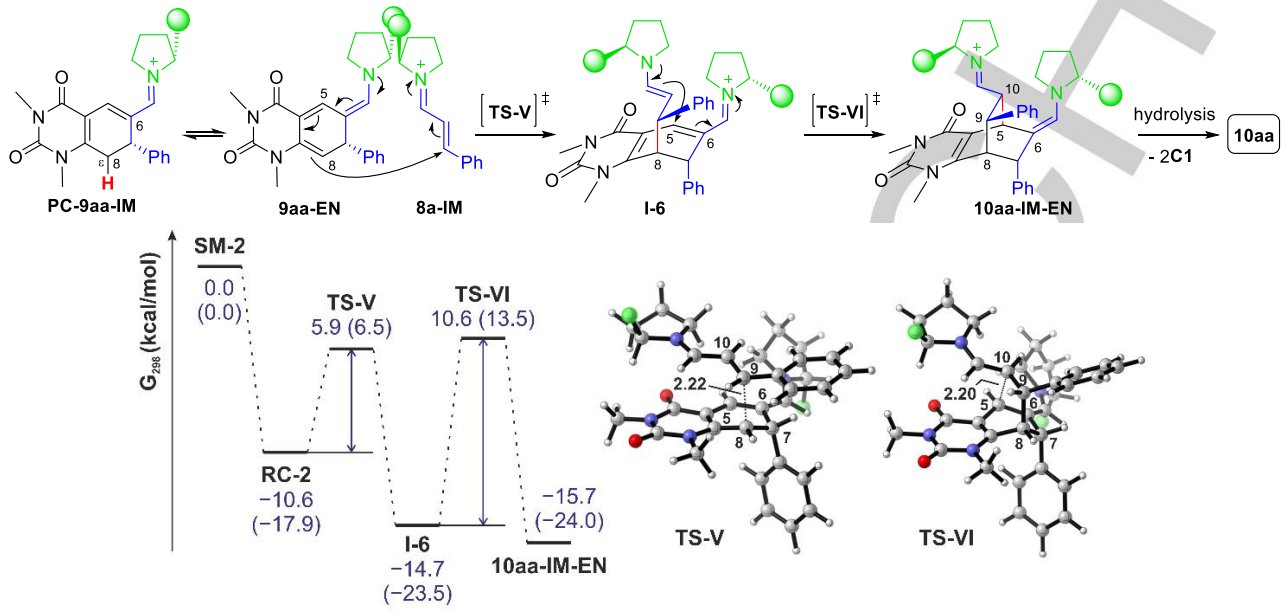

Chart 3. Reaction scheme (above) and reaction profile (below) for the addition of **9aa-EN** to **8a-IM**. Free energy profiles (kcal·mol^{-1}) in the gas-phase at the M06-2X/6-31G(d) level of theory. Energies in parentheses are relative to single point calculations at the M06-2X/6-311++G(d,p) level of theory in CH_2Cl_2. **SM-2**: separated reactants at infinite distance (**9aa-EN** + **8a-IM**); **RC**: reactant complex; **TS**: transition state; **I**: intermediate. Transition state **TS-V** (addition reaction) and **TS-VI** (cyclization reaction); distances in Angstrom. Silylated diphenylmethanol group is represented as a green sphere.

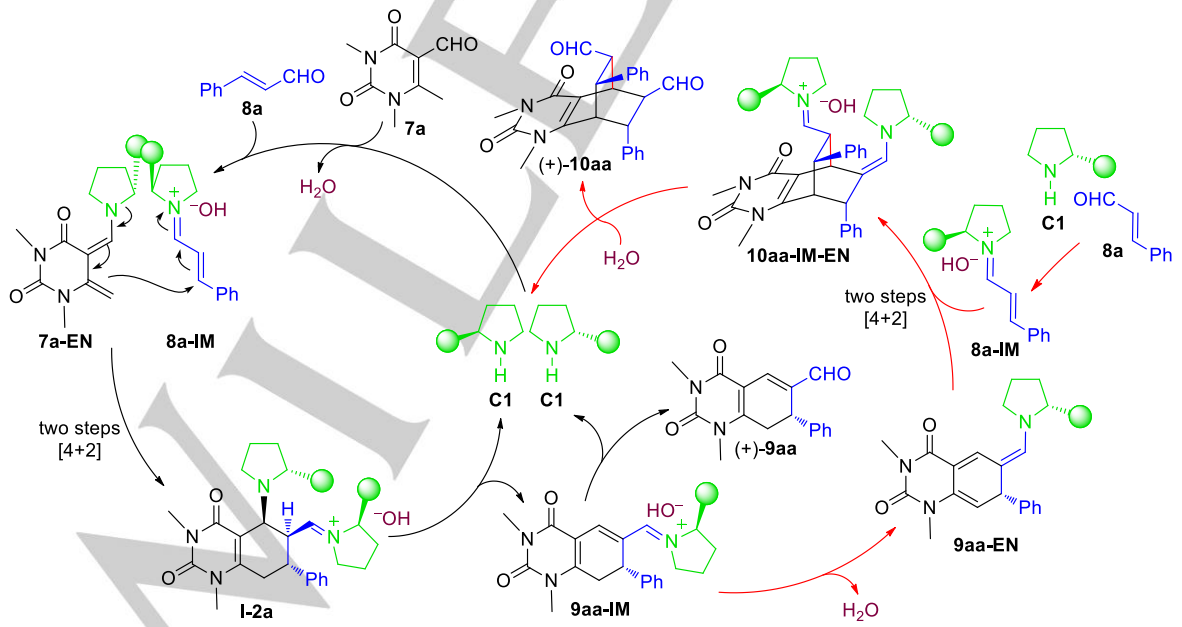

Scheme 5. Organocatalytic homo-synergistic cycles 1 (black arrows) and 2 (red arrows) accounting for the chemodivergent synthesis of bicycles **9** and tricycles **10** in this study.

Conclusion

A novel method has been developed, which allowed the rapid transformation of easily accessible and low-cost uracil substrates of type **7** to new three-dimensional carbocycle-fused uracils. The rationale behind this endeavor was simple: installation of a carbaldehyde functional group at the C5 site of 6-methyluracil (as in uracils **7**) would enhance the remote enolization at the vinylogous C6-methyl site, favor the formation of a reactive *o*QDM species (an activated diene) for [4 + 2] coupling to an enal acceptor (dienophile), while providing a possible appendage for the covalent activation by the amine catalyst. The hypothesis was confirmed by real-world chemistry and, upon optimized mild reaction conditions, the route proved practical and chemodivergent, providing access to two distinct small collections of products in good yields and almost complete enantioselectivities namely, bicyclic compounds **9** and tricyclic products **10**, remarkably featuring six contiguous stereocenters.
Detailed DFT calculations and control experiments clarified the role of the silylprolinol catalyst, which *solely and concomitantly* activates both enal substrates and orchestrates the overall transformation. Mechanistically, a first organocatalyzed stepwise eliminative [4 + 2] cross cycloaddition between the carbaldehyde substrates leads to a bicyclic iminium ion intermediate (**PC-9aa-IM**), which divergently turns into bicyclic targets **9** by hydrolysis, or converts to tricyclic targets **10** via a further trienamine-mediated stepwise [4 + 2] cycloaddition, depending upon the reaction conditions.
We anticipate that this robust and simple chemical transformation will serve to widen sampling of three-dimensional chemical space around the key uracil core.

Acknowledgements

This work was supported by Regione Autonoma della Sardegna (RASSR81788, 2017, “Green Chemistry in Drug Discovery - sintesi sostenibili di nuovi inibitori di telomerase”) and by Università di Parma (ZNRFNC_RICERCA_IST). G.P. wishes to thank Chiesi Farmaceutici S.p.A. for the use of D8Venture diffractometer. Thanks are due to Centro Interdipartimentale Misure “G. Casnati” (Università di Parma, Italy) for instrumental facilities. We thank M. Cito (Department of Food and Drug, University of Parma) for Karl Fischer titration measurements.

Keywords: asymmetric synthesis • fused-ring systems • heterocycles • organocatalysis • vinylogy

[1] Y. Qin, L. Zhu, S. Luo, *Chem. Rev.* **2017**, *117*, 9433–9520.
[2] D. C. Blakemore, L. Castro, I. Churcher, D. C. Rees, A. W. Thomas, D. M. Wilson, A. Wood, *Nat. Chem.* **2018**, *10*, 383–394.
[3] T. L. P. Galvão, I. M. Rocha, M. D. M. C. Ribeiro da Silva, M. A. V. Ribeiro da Silva, *J. Phys. Chem. A* **2013**, *117*, 5826–5836.
[4] S. I. Zav'yalov, G. I. Ezhova, N. E. Kravchenko, L. B. Kulikova, O. V. Dorofeeva, E. E. Rumyantseva, A. G. Zavozin, *Pharm. Chem. J.* **2003**, *37*, 337–341.
[5] a) E. De Clercq, *J. Med. Chem.* **2019**, *62*, 7322–7339; b) A. Pałasz, D. Cież, *Eur. J. Med. Chem.* **2015**, *97*, 582–611.
[6] M. I. Lin, B. H. Su, C. H. Lee, S. T. Wang, W. C. Wu, P. Dangate, S. Y. Wang, W. I. Huang, T. J. Cheng, O. A. Lin, Y. S. E. Cheng, Y. J. Tseng, C. M. Sun, *Eur. J. Med. Chem.* **2015**, *102*, 477–486.
[7] C. Curti, L. Battistini, A. Sartori, F. Zanardi, *Chem. Rev.* **2020**, *120*, 2448–2612, and references therein.
[8] a) B. Yang, S. Gao, *Chem. Soc. Rev.* **2018**, *47*, 7926–7953; b) B.-X. Xiao, X.-Y. Gao, W. Du, Y.-C. Chen, *Chem. Eur. J.* **2019**, *25*, 1607-1613.
[9] Y. Liu, M. Nappi, E. Arceo, S. Vera, P. Melchiorre, *J. Am. Chem. Soc.* **2011**, *133*, 15212–15218.
[10] a) G. Rassu, C. Curti, V. Zambrano, L. Pinna, N. Brindani, G. Pelosi, F. Zanardi, *Chem. Eur. J.* **2016**, *22*, 12637–12640; b) N. Brindani, G. Rassu, L. Dell'Amico, V. Zambrano, L. Pinna, C. Curti, A. Sartori, L. Battistini, G. Casiraghi, G. Pelosi, D. Greco, F. Zanardi, *Angew. Chem.* **2015**, *127*, 7494-7498; *Angew. Chem. Int. Ed.* **2015**, *54*, 7386–7390; c) for a recent review on this topic see: C. Curti, A. Sartori, L. Battistini, F. Zanardi, *Synlett* **2018**, *29*, 266–281.
[11] T. Li, J. Zhu, D. Wu, X. Li, S. Wang, H. Li, J. Li, W. Wang, *Chem. Eur. J.* **2013**, *19*, 9147–9150.
[12] Interestingly, the presence of lipophilic MOM, MEM, and BOM groups at N1/N3 uracil moiety highly impacted the physical properties of both the starting substrates **7** and products **9**, which in fact proved much more soluble in organic solvents as compared to the dimethyl-protected counterparts.
[13] Deposition Number CCDC 1995936 contains the supplementary crystallographic data for this paper. These data are provided free of charge by the joint Cambridge Crystallographic Data Centre and Fachinformationszentrum Karlsruhe Access Structures service www.ccdc.cam.ac.uk/structures.
[14] a) B.J. Bench, C. Liu, C.R. Evett, C.M.H. Watanabe, *J. Org. Chem.* **2006**, *71*, 9458–9463; b) C. Grondal, M. Jeanty, D. Enders, D. *Nat. Chem.* **2010**, *2*, 167–178; c) N. Hammer, L.A. Leth, J. Stiller, M.E. Jensen, K.A. Jørgensen, *Chem. Sci.* **2016**, *7*, 3649-3657; d) S. Meninno, M. Meazza, J.W. Yang, T. Tejero, P. Merino, R. Rios, *Chem. Eur. J.* **2019**, *25*, 7623–7627.
[15] DFT computational investigation of the relevant reactions involved in this work was carried out at the M06-2X/6-311++g(d,p) IEFPCM (CH2Cl2)//M06-2X/6-31G(d) level of theory. For details, see Supporting Information.
[16] S. Bahmanyar, K.N. Houk, *J. Am. Chem. Soc.* **2001**, *123*, 11273-11283.
[17] Water content in commercial benzoic acid used in this work, either as a solid or in CH_2Cl_2 solution, was determined via Karl Fischer titration (KF) and resulted 0.53% and 0.02%, respectively. Also, reaction of **7a** and **8a** with H_2O (7.0 equiv) and in the absence of benzoic acid led to the almost exclusive formation of **9aa**; these experiments allowed us to exclude an active role of water in controlling chemoselectivity. Interestingly, KF titration of a control reaction between **7a** and **8a** (under the optimized conditions in Table 1, entry 14) revealed the formation of water (0.5 equiv) after 12 hours (ca 50% conversion), thus confirming the proposed catalytic cycle shown in Scheme 5, where 1 equiv of water is formed in either catalytic cycle. We thank a reviewer for drawing this point to our attention.

10.1002/anie.202007509

WILEY-VCH

RESEARCH ARTICLE

Entry for the Table of Contents

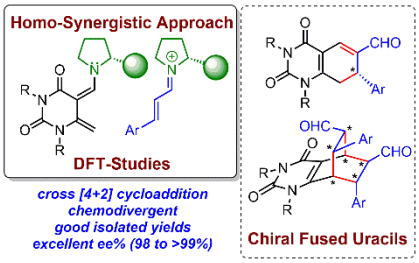

In synergy to diverge. Cross [4 + 2] cycloadditions between uracil-based aldehydes and β-aryl enals were carried out under mild conditions in the presence of the popular diphenylsilyl-protected prolinol organocatalyst, which provided homo-synergistic activation of both substrates. Bicyclic and tricyclic fused uracils were chemodivergently forged in good yields and maximum levels of enantioselectivity.

Università di Parma Twitter username: @unipr